ATTRIBUTION OF THE PERSISTENT SPRING–SUMMER HOT AND DRY EXTREMES OVER NORTHEAST CHINA IN 2017

Shanshan Wang, Xing Yuan, and Renguang Wu

Anthropogenic climate change has increased the risk of 2017 northeast China persistent spring–summer hot and dry extremes by 5%–55% and 37%–113% respectively.

INTRODUCTION. In March–July 2017, northeast China suffered a long period of intense hot and dry weather. This concurrent heat and drought extreme event affected more than 7.4×10^5 km^2 of crops and herbage, especially over Xilinguole and Hulunbuir Prairie, and resulted in a direct economic loss of about 70 billion renminbi (RMB) (about 10 billion U.S. dollars; Zhang et al. 2017). During this period, northeast China was under the influence of a persistent and extensive anticyclone centered around Lake Baikal (the Baikal high). Another remarkable fact is that 2017 was the third warmest year on record (WMO 2018), with the absence of El Niño conditions. Meanwhile, the Arctic sea ice extent was well below average during the preceding winter and spring, especially in the Barents Sea and its adjacent seas (WMO 2017).

The increase of greenhouse gases is likely responsible for the warming temperature and the enhancing anticyclone around Lake Baikal in recent decades, especially after the 1970s (Zhu et al. 2012). Meanwhile, Arctic sea ice variability is a possible factor for triggering the overlying atmospheric circulation anomalies with a lagged effect, such as sustaining the Eurasian teleconnection pattern and the Baikal high system through land–air interaction (e.g., Zhao et al. 2004; Li et al. 2018; Zhang et al. 2018), thereby affecting the climate variations over northeast China (e.g., Wu et al. 2009; Wang et al. 2017; Li et al. 2018).

Therefore, in addition to assessing the contributions of anthropogenic climate change on the persistent hot and dry extremes in March–July of 2017 over northeast China, we also briefly discuss the mechanism for the occurrence of the concurrent extremes from the perspective of the changing Baikal high.

DATA AND METHODS. Monthly surface air temperature (T2M) and precipitation (PRE) observations at 839 stations provided by the National Meteorological Information Center (NMIC) at the China Meteorological Administration (CMA) were bilinearly interpolated into 1° grid cells for the period 1951–2017. Because there were limited observation stations before 1960 and the historical attribution simulations from phase 5 of the Coupled Model Intercomparison Project (CMIP5; Taylor et al. 2012) ended in 2005, T2M and PRE anomalies were calculated relative to the 1960–2005 climatology. The generalized extreme value (GEV) distribution was used to fit the March–July mean T2M and PRE distribution and to estimate the return period excluding the year 2017 in this study.

To analyze the possible reasons for the 2017 concurrent hot and dry extreme event, monthly sea ice area fraction (SIC) data from the Met Office Hadley Centre during 1870–2017 (Rayner et al. 2003) at 1° resolution were used in this study. Monthly mean 500-hPa geopotential height (HGT500) during 1979–2017 at 2.5° resolution was derived from the ERA-Interim reanalysis (Dee et al. 2011). The Baikal

AFFILIATIONS: Wang—Key Laboratory of Arid Climatic Change and Reducing Disaster of Gansu Province, and Key Open Laboratory of Arid Climate Change and Disaster Reduction, Institute of Arid Meteorology, China Meteorological Administration, Lanzhou, China; Yuan— School of Hydrology and Water Resources, Nanjing University of Information Science and Technology, Nanjing, Jiangsu, and Key Laboratory of Regional Climate–Environment for Temperate East Asia (RCE-TEA), Institute of Atmospheric Physics, Chinese Academy of Sciences, Beijing, China; Wu—Center for Monsoon System Research, Institute of Atmospheric Physics, Chinese Academy of Sciences, Beijing, China
CORRESPONDING AUTHOR: Xing Yuan, yuanxing@tea.ac.cn

DOI:10.1175/BAMS-D-18-0120.1

A supplement to this article is available online (10.1175/BAMS-D-18-0120.2)

high intensity was defined as the mean HGT500 averaged over the region of 80°–120°E and 40°–70°N (Chen et al. 2013) during March–July.

Monthly T2M and PRE simulations from multiple CMIP5 models driven by all (ALL) and natural only (NAT) forcings during 1950–2005 were used in this study (see Table ES1 in the online supplemental information for the model list and information). All simulations were bilinearly regridded into 1° resolution and matched well with the observed distribution via a Kolmogorov–Smirnov test ($p < 0.05$). Because of the data availability, only one pair of realizations (r1i1p1) were used to assure an equal weight for different CMIP5 models. The fraction of attributable risk (FAR; Stott et al. 2004) method, which compares the event tail probabilities (P) between the CMIP5/NAT and CMIP5/ALL simulations ($\mathrm{FAR} = 1 - P_{\mathrm{NAT}}/P_{\mathrm{ALL}}$), and the probability ratio ($\mathrm{PR} = P_{\mathrm{ALL}}/P_{\mathrm{NAT}}$; Fischer and Knutti 2015) were both used to assess the contributions of anthropogenic climate change. FAR is the fractional contribution of human activity to a particular event, and PR is the factor by which the probability of an event has changed under anthropogenic forcing (Ma et al. 2017). Bootstrapping was performed 1000 times to estimate the FAR and PR uncertainty (Yuan et al. 2018a). To identify the significance level of the difference between ALL and NAT forcings for a given period, p values were calculated using the block bootstrap resampling approach of Singh et al. (2014). In addition, the CMIP5 model-simulated HGT500 was also used here.

In this paper, the highest 25% of regional mean T2M anomalies during each March–July were considered as the extreme hot events (as are the Baikal high intensity extremes), and the lowest 25% of the regional mean PRE anomalies were considered as the extreme dry events. If both extremes occurred in the same year (e.g., 2017), it was considered as a concurrent hot and dry extreme event.

RESULTS. Figure 1a shows the spatial distribution of March–July mean T2M anomaly during 2017. Northeast China experienced a much hotter spring and summer than normal, with anomalies exceeding 2°C over most regions. The area-averaged temperature anomaly in March–July 2017 is ranked as the first during the most recent 67 years according to the CMA/NMIC observations (Fig. 1c), with a return period of 245 years (Fig. 1e). Meanwhile, the extensive rainfall deficit occurred across northeast China (Fig. 1b), and the area-averaged rainfall anomaly in March–July 2017 was unprecedentedly low (Fig. 1d), 36% less than normal with a return period of 122 years (Fig. 1e).

The concurrent hot and dry extremes over northeast China occurred without a strong El Niño–Southern Oscillation (ENSO) signal, but in the context of record-breaking continuing global warmth of 2015–17 and the unprecedentedly low Arctic sea ice extent in the preceding winter and spring (WMO 2017, 2018). As seen from the associated circulation pattern, northeast China was dominated by a sustained anticyclone centered around Lake Baikal during this period (Fig. 1f), which lasted from March to July of 2017. Meanwhile, there were anomalous low pressure centers in both upstream (Ural Mountains) and downstream (northwest Pacific Ocean) regions. Influenced by this circulation pattern, northeast China was behind the deepened East Asian trough and before the enhanced Baikal ridge, and therefore the descending movement and the northwesterly in the upper level were prevailing, which was favorable for the abnormal hot and dry extremes (Wang et al. 2017). Meanwhile, it is also found that HGT500 exhibited a significant enhancing trend around Lake Baikal (Fig. 1g), which implies that the Baikal high has been intensifying during the past 40 years (Fig. 1h).

As mentioned in the introduction, anthropogenic warming enhances the Baikal high (Zhu et al. 2012). Meanwhile, there exists a noticeable lagged relationship between the Arctic sea ice in preceding winter and spring (particularly in spring) and the midlatitudinal circulation of Eurasia in following seasons via singular value decomposition (SVD) analysis (see Fig. ES1). As for the interannual variations, less preceding Arctic sea ice, particularly in the Barents Sea and its adjacent seas, corresponds to anomalously high pressure around Lake Baikal in the next spring and summer statistically. The lagged relationship increases significantly after 1997 ($p < 0.05$; see Fig. ES2). Recently, such a lagged effect between the Eurasian mid- to high-latitude teleconnection in summer and the interannual variations of Arctic sea ice from preceding spring to summer was also confirmed by model simulations (Li et al. 2018; Zhang et al. 2018).

To attribute the concurrent hot and dry extremes in March–July of 2017, CMIP5 model simulations with all and natural only forcings were used. Here, the probability density functions (PDFs) for extreme hot (dry) defined as those exceeding 75% (less than 75%) percentiles of the observed mean March–July T2M (PRE) averaged over northeast China were calculated by fitting GEV distributions. The FAR and PR for the March–July mean T2M hotter than 2017 is 0.23 (±0.17) and 1.30 (0.25), with the return period decreased from 22 years to 17 years under the influence of the

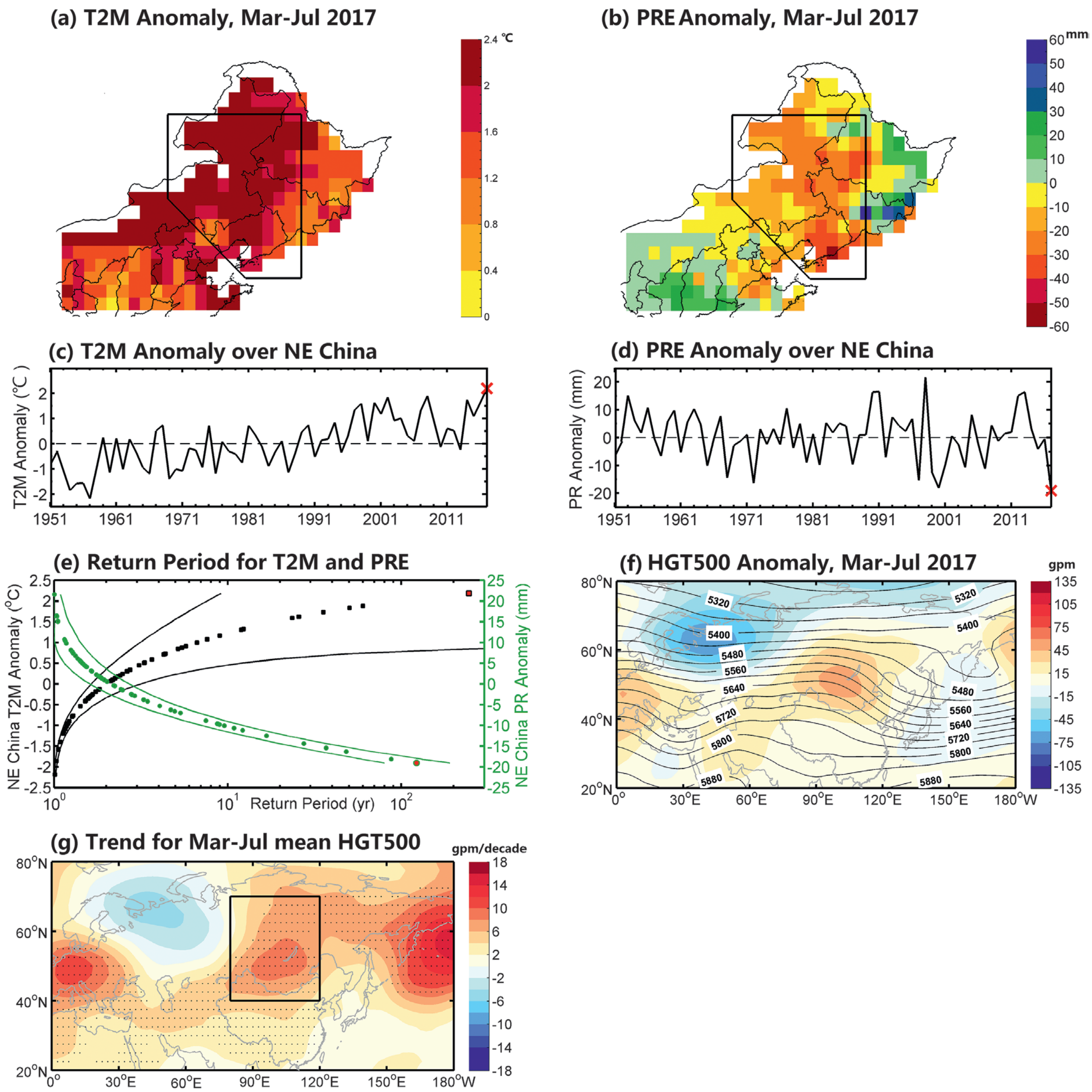

Fig. 1. (a) Temperature (T2M) anomaly (°C) and (b) precipitation (PRE) anomaly (mm) during March–July of 2017 relative to the 1960–2005 climatology based on CMA/NMIC station observations. (c),(d) Observed regional mean T2M and PRE anomalies averaged over northeast China. (e) Return periods and 95% confidence intervals for regional mean March–July T2M and PRE anomalies, where the red dots represent year 2017. (f) 500-hPa geopotential height (gpm; contours) and its anomalies (gpm; shading). (g) Trends for 500-hPa geopotential height (gpm decade^{-1}) during 1979–2017, where the stippling indicates a 95% confidence level (p < 0.05) using the Mann–Kendall test.

anthropogenic climate change (Fig. 2a). There is no significant trend for the March–July mean PRE in CMIP5 simulations (not shown), which is consistent with the observation (Fig. 1d). However, the likelihood for low precipitation extremes like than in 2017 significantly increased under anthropogenic influence, with FAR and PR values of 0.43 (±0.12) and 1.75 (±0.38) respectively (Fig. 2b). Meanwhile, the frequency of the concurrent hot and dry extremes shows a visible increasing trend since the mid-1960s in ALL simulations, and the associated FAR values were positive all the time during the CMIP5 historical simulation period (Fig. 2c). In particular, ALL and NAT simulated concurrent hot and dry events were found to be different at 0.001 significance level during the most recent 30-yr period, with a FAR value of 0.22–0.25 (Fig. 2c).

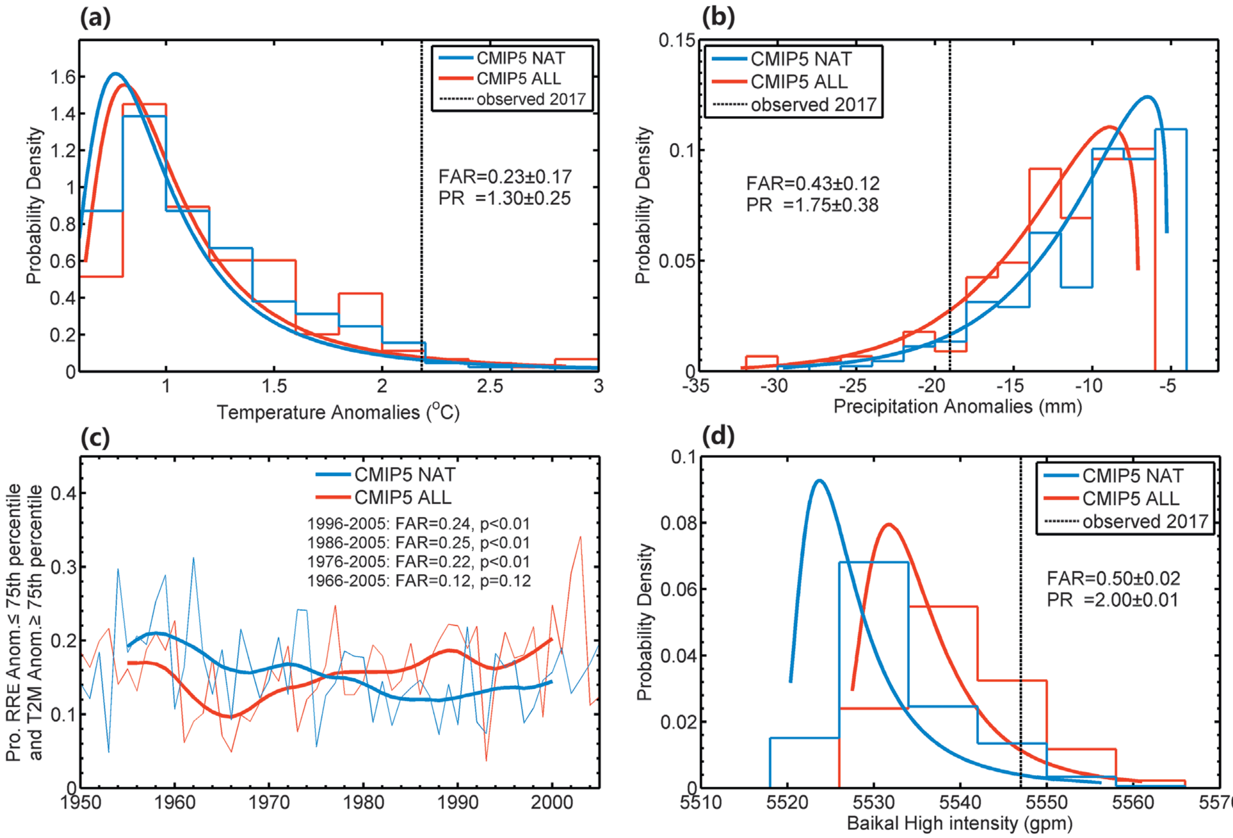

FIG. 2. Histogram (bars) and probability density functions (PDFs; curve) for northeast China March–July mean (a) temperature extremes and (b) precipitation extremes from CMIP5 simulations under all (ALL) and natural only (NAT) forcings during 1950–2005. (c) The probability of concurrent extremely low precipitation and high temperature. The bold curves show 11-yr running mean of the annual time series. (d) As in (a) and (b), but for the Baikal high intensity extremes (gpm).

The related strong Baikal high extremes of such concurrent hot and dry extreme events over northeast China were also examined with ALL and NAT simulations (Fig. 2d). The likelihood of an extremely strong Baikal high like that of 2017 increased due to anthropogenic climate forcing, with FAR and PR values of 0.5 (±0.02) and 2.0 (±0.01).

CONCLUSIONS. In 2017, persistent spring–summer hot and dry extremes hit northeast China, characterized by the highest temperature on record and the unprecedentedly low precipitation. Observational analysis showed that the extensive and sustained Baikal high played a crucial role in this extreme event, which was possibly contributed to by anthropogenic global warming and deceasing Arctic sea ice in preceding winter and spring. By analyzing CMIP5 model simulations, it is found that the likelihood of northeast China extremely high temperature such as that occurred in 2017 increased by about 30% due to anthropogenic climate change, and the likelihood of extremely low precipitation increased by about 75% although its mean value showed no robust trend. Furthermore, the concurrency of such hot and dry extremes exhibited an increasing risk of 28% in the recent 30-yr period due to anthropogenic climate change.

We conjectured that the increasing risk of 2017 persistent spring–summer hot and dry extremes over northeast China was related to the enhancing Baikal high, whose likelihood was doubled in a warming climate. By analyzing pentad-mean soil moisture and temperature, Yuan et al. (2018b) reported an intensification of concurrent hot and dry extreme events over southern Africa due to anthropogenic climate change, which suggests that increasing concurrent extreme events could be very likely without any mitigation strategies.

ACKNOWLEDGMENTS. We acknowledge the World Climate Research Programme's Working Group on Coupled Modeling, which is responsible for CMIP. This work was supported by National Key R&D Program of China (2018YFA0606002), the Natural Science Foundation of China (41605055, 41630426), and the China Special Fund for Meteorological Research in the Public Interest (Major projects) (GYHY201506001).

REFERENCES

Chen, D., C. Bueh, and K. Y. Zhu, 2013: Interannual and interdecadal variabilities of circulation over Lake Baikal region in late spring and their association with temperature and precipitation over China (in Chinese). *Chin. J. Atmos. Sci.*, **37**, 1199–1209.

Dee, D. P., and Coauthors, 2011: The ERA-Interim reanalysis: Configuration and performance of the data assimilation system. *Quart. J. Roy. Meteor. Soc.*, **137**, 553–597, https://doi.org/10.1002/qj.828.

Fischer, E. M., and R. Knutti, 2015: Anthropogenic contribution to global occurrence of heavy-precipitation and high-temperature extremes. *Nat. Climate Change*, **5**, 560–564, https://doi.org/10.1038/nclimate2617.

Li, H., H. Chen, H. Wang, J. Sun, and J. Ma, 2018: Can Barents Sea ice decline in spring enhance summer hot drought events over northeastern China? *J. Climate*, **31**, 4705–4725, https://doi.org/10.1175/JCLI-D-17-0429.1.

Ma, S. M., T. J. Zhou, D. A. Stone, O. Angélil, and H. Shiogama, 2017: Attribution of the July–August 2013 heat event in central and eastern China to anthropogenic greenhouse gas emissions. *Environ. Res. Lett.*, **12**, 054020, https://doi.org/10.1088/1748-9326/aa69d2.

Rayner, N. A., D. E. Parker, E. B. Horton, C. K. Folland, L. V. Alexander, D. P. Rowell, E. C. Kent, and A. Kaplan, 2003: Global analyses of sea surface temperature, sea ice, and night marine air temperature since the late nineteenth century. *J. Geophys. Res.*, **108**, 4407, https://doi.org/10.1029/2002JD002670.

Singh, D., M. Tsiang, B. Rajaratnam, and N. S. Diffenbaugh, 2014: Observed changes in extreme wet and dry spells during the South Asian summer monsoon season. *Nat. Climate Change*, **4**, 456–461, https://doi.org/10.1038/nclimate2208.

Stott, P. A., D. A. Stone, and M. R. Allen, 2004: Human contribution to the European heatwave of 2003. *Nature*, **432**, 610–614, https://doi.org/10.1038/nature03089.

Taylor, K. E., R. J. Stouffer, and G. A. Meehl, 2012: An overview of CMIP5 and the experiment design. *Bull. Amer. Meteor. Soc.*, **93**, 485–498, https://doi.org/10.1175/BAMS-D-11-00094.1.

Wang, S., X. Yuan, and Y. Li, 2017: Does a strong El Niño imply a higher predictability of extreme drought? *Sci. Rep.*, **7**, 40741, https://doi.org/10.1038/srep40741.

WMO, 2017: WMO Statement on the State of the Global Climate in 2016. World Meteorological Organization, 24 pp., https://public.wmo.int/en/resources/library/wmo-statement-state-of-global-climate-2016.

——, 2018: WMO Statement on the State of the Global Climate in 2017. World Meteorological Organization, 35 pp., https://public.wmo.int/en/resources/library/wmo-statement-state-of-global-climate-2017.

Wu, B., R. Zhang, B. Wang, and R. D'Arrigo, 2009: On the association between spring Arctic sea ice concentration and Chinese summer rainfall. *Geophys. Res. Lett.*, **36**, L09501, https://doi.org/10.1029/2009GL037299.

Yuan, X., S. Wang, and Z.-Z. Hu, 2018a: Do climate change and El Niño increase likelihood of Yangtze River extreme rainfall? [in "Explaining Extreme Events of 2016 from a Climate Perspective"]. *Bull. Amer. Meteor. Soc.*, **99**, S113–S117, https://doi.org/10.1175/BAMS-D-17-0089.1.

——, L. Wang, and E. F. Wood, 2018b: Anthropogenic intensification of southern African flash droughts as exemplified by the 2015/16 season [in "Explaining Extreme Events of 2016 from a Climate Perspective"]. *Bull. Amer. Meteor. Soc.*, **99**, S86–S90, https://doi.org/10.1175/BAMS-D-17-0077.1.

Zhang, Y., L. Zhang, S. P. Wang, and J. Feng, 2017: Drought events and their influence in summer of 2017 in China (in Chinese). *J. Arid Meteor.*, **35**, 899–905.

Zhao, P., X. Zhang, X. Zhou, M. Ikeda, and Y. Yin, 2004: The sea ice extent anomaly in the North Pacific and its impact on the East Asian summer monsoon rainfall. *J. Climate*, **17**, 3434–3447, https://doi.org/10.1175/1520-0442(2004)017<3434:TSIEAI>2.0.CO;2.

Zhu, C., B. Wang, W. Qian, and B. Zhang, 2012: Recent weakening of northern East Asian summer monsoon: A possible response to global warming. *Geophys. Res. Lett.*, **39**, L09701, https://doi.org/10.1029/2012GL051155.